Evaluating Integrity and Continuity Risks of Cycle Resolution in the Presence of Receiver Faults

Samer Khanafseh, Steven Langel, Mathieu Joerger and Boris Pervan
Illinois Institute of Technology, Chicago, IL

ABSTRACT

This paper introduces a method to detect reference receiver faults and compute an upper bound on integrity and continuity risks. In high accuracy aviation applications, differential carrier phase navigation algorithms are used, and carrier phase cycle ambiguities must be estimated and resolved as integers (or 'fixed ambiguities'). In applications that also demand high integrity, the cycle resolution process must comply with integrity risk requirements. Under normal measurement error conditions, fault-free integrity risk can readily be quantified using existing cycle resolution methods. One source of integrity risk is the potential for GPS reference receiver failure. Integrity risk in these situations is typically mitigated by equipping the reference station with redundant receivers. In this work, we develop a method using multiple receivers to quantify integrity and continuity risks for algorithms that rely on cycle resolution in the presence of reference receiver faults.

INTRODUCTION

Carrier phase measurements can be used to provide high accuracy estimates of a user's position. For life-critical GNSS applications, such as civil aircraft approach with a Ground Based Augmentation System (GBAS), extremely high levels of integrity are required. For example, for a Category I system, a maximum integrity risk of the order of 10^{-7} per aircraft approach is required with a vertical position alert limit of 10 m. However, the accuracy requirements for the GBAS application (vertical 95% accuracy on the order of 2 m) are not stringent enough to require the use of high precision carrier phase navigation [1]. With the emergence of new aviation applications [2 – 6], where human life is involved and the vehicles are highly dynamic, high levels of both integrity and accuracy are required simultaneously. In these situations, the use of carrier phase measurements becomes necessary. Also, in order to achieve centimeter-level positioning accuracy using carrier phase measurements, the resolution of cycle ambiguities is required.

The integrity of the navigation system is at risk when a reference receiver fails. For the purpose of this work, a receiver fault is defined as an event on which a receiver produces anomalous measurements from either single or multiple channels. These scenarios are usually handled by equipping the reference station with multiple receivers, which provide redundancy for estimation and a means for reference receiver fault mitigation. Although multiple reference receivers are usually used for integrity, it is possible to utilize these redundant measurements to enhance accuracy as well [7]. The improvement in accuracy that is achievable depends heavily on how these measurements are combined. In this work, we use the range domain coupled estimation approach, where measurements from all reference receivers are coupled with airborne measurements in the range domain and used to estimate a unified solution.

Fault-free integrity risk is typically defined as the probability that the position error exceeds predefined alert limits. In applications where integrity and accuracy requirements are stringent, it is necessary to quantify the impact of the cycle resolution process on position domain integrity. In this context, the bootstrap fixing method is used as a baseline for cycle resolution because it provides an a priori success rate (probability of correct fix) [8].

Two separate types of probabilities must be calculated when evaluating the integrity risk of cycle resolution. The first is the probability of correct fix and the second probability is computed from the distribution of the position estimate error conditioned on the fixed solution. Both of these probability types are strongly influenced by rare-event measurement faults. Several publications address the computation of the probability of correct fix in the presence of measurement biases (for example, see [9]). However, these methods are only applicable if the bias on the measurement error is exactly known. In previous work [10] we developed a method to compute an

upper bound on cycle resolution integrity risk in the presence of bounded measurement errors and faults. For example, in the case of atmospheric anomalies, the magnitude of the measurement error is never exactly known, but it can often be physically bounded [11]. In contrast, reference receiver faults have no established threat models and therefore, cannot be bounded.

Overall, the integrity risk of the navigation system must comply with the integrity risk requirement under the fault-free hypothesis (H0), the single-receiver-failure hypothesis (H1) and all other failure hypotheses (H2). The H0 and H1 hypotheses are the main focus of this paper, and therefore all other failure hypotheses (multi-receiver failures, signal in space failures, etc.) will not be discussed. Although the literature provides solutions for integrity under the H1 hypothesis for snapshot navigation systems (such as GBAS) [1, 12, 13], H1 integrity monitoring and analysis for carrier phase navigation algorithms has not been discussed previously. As we will show in this paper, the necessity of estimating and resolving the cycle ambiguities is the main challenge in evaluating H1 integrity for high accuracy carrier phase navigation applications.

In this paper, we derive a method to simultaneously account for the effects of reference receiver failures on position estimate error and cycle ambiguity resolution. This derivation directly leads to two approaches to bounding integrity and continuity risk: the first is simpler to implement, but provides a loose bound; the second approach, although more complex, provides a much tighter bound. Finally we quantify the performance of the two bounding methods for an example navigation application.

H1 HYPOTHESIS MITIGATION ALGORITHM

The H1 hypothesis is defined as a fault associated with any one, and only one, reference receiver. A fault includes any anomalous measurement that is not immediately detected by the reference station. Therefore, the broadcast reference data are affected, which in turn, induces errors in the airborne navigation system. In this work, the reference receiver mitigation algorithm will be based on the GBAS H1 algorithm [1, 12, 13]. However, because of the differences between the navigation algorithms in the two systems, significant modifications are required. For example, the GBAS navigation algorithm is a snapshot estimation system that uses smoothed pseudorange measurements and estimates the user position with respect to the reference receivers by a least squares estimation process [1]. In contrast, the navigation systems considered in this paper are based on carrier phase differential GPS positioning [2-6]. They might use additional filtering for different measurement observables (such as ionospheric-free or geometry-free observables). In addition, to reach the desired accuracy level, cycle ambiguities are usually either completely or partially fixed subject to the integrity risk requirement. As we will see in this paper, all of these complexities in the fault-free navigation algorithm present tremendous challenges compared to the existing GBAS solution in the H1 mitigation for the navigation algorithm.

Since receiver faults have a direct impact on the measurements coming out of the receivers, it might be intuitive to design a monitor to detect faults directly at the measurement level. Examples of such monitors include Receiver Autonomous Integrity Monitor (RAIM) [14, 15], which can be implemented on the aircraft or a B-Value monitor [13], which can be implemented on the reference station. Typically these monitors use a threshold to detect the failure that is derived based on the type of monitor, measurement error characteristics and system continuity requirements (i.e., probability of false alarm). In principle, such a monitor will pass erroneous measurements that are smaller than the derived threshold to the airborne system without taking into account the after-effect of such anomalous measurements on the airborne position estimate. Usually, the impact is analyzed by running a separate analysis to determine if the system still meets the requirements in the presence of reference measurement anomalies. For airborne processes that include filtering and cycle resolution, this requires defining the receiver fault threat space – a task that requires rigorous effort. Since different receivers might fail differently in regards to the magnitude and shape of the fault, even under the assumption that all kinds of faults have been considered for one receiver, the threat space analysis might only apply to that specific kind of receiver. In addition, the complex airborne architecture might include a rounding process for cycle ambiguity resolution. Unlike most linear filtering processes that are used in the airborne navigation architecture, the rounding operation is nonlinear. Therefore, performing offline analysis to determine the effectiveness of the monitor is not possible using traditional covariance analysis. The alternative is to use a Monte-Carlo simulation, which, due to the span of the potential threat space and sensitivity of the resulting position error to satellite geometry, is a highly impractical method to prove compliance with tight integrity requirements of 10^{-7} for example. Instead, reference receiver failures are best detected in the position domain at the aircraft. Since the reference station has no access to the airborne measurements, airborne filtering durations, or how many ambiguities have been fixed (if partial fixing is used), it is essentially impossible for the reference station to predict the effect of an undetected reference receiver fault on the aircraft position estimate. As a result, the airborne system ultimately must be responsible for mitigating the position domain impact of reference receiver faults.

In fault detection algorithms, it is a common practice to compute a test statistic and compare it to a predefined threshold. In receiver failure detection, as we will see shortly, the protection level and the alert limit mimic the test statistics and the threshold, respectively. The alert limit is a containment limit requirement representing the maximum tolerable vertical position error. The protection level is defined as a statistical overbound of the vertical position errors and is derived from the associated integrity risk allocation. In this context, the probability of hazardously misleading information P(*MI*) (equivalent to the integrity risk) is defined as the probability that the position error exceeds the alert limit due to H0 and H1 hypotheses only. H2 hypothesis (events not covered by H0 or H1 such as ranging source faults and simultaneous multiple reference receiver faults) are allocated a separate budget, $P(H_2)$, from the total integrity risk. Since the H0 and H1 hypotheses are mutually exclusive and exhaustive events and assuming the reference station is equipped with *M* receivers (each is possible to fail), *P*(*MI*) can be written as,

$$P(MI) = P(MI|H_0)P(H_0) + \sum_{j=1}^{M} P(MI|H_{1j})P(H_{1j}) \quad (1)$$

where,
$P(\mathrm{H}_0)$ is the fault free probability
$P(\mathrm{H}_{1\mathrm{j}})$ is the probability of failure for reference receiver *j*

In order to compute protection levels, an integrity risk requirement (I_{req}) needs to be allocated for the fault free hypothesis $I_{H0,req}$ and all *M* $I_{H1j,req}$ hypotheses in (1) as illustrated in Figure 1. This allocation can be either equally distributed or optimized for best performance.

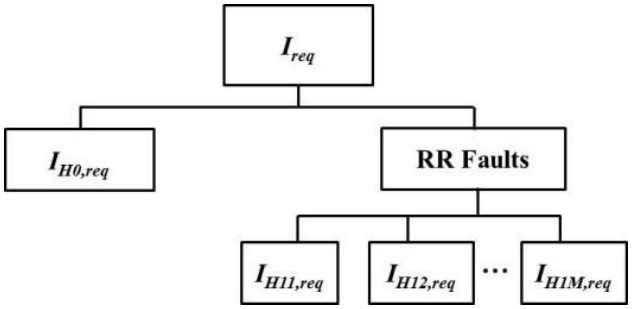

Figure 1 Integrity risk allocation tree

If the position estimation algorithm relies on cycle resolution, the hypothesis that the cycle ambiguities have been fixed incorrectly must be taken into account. Therefore, using the law of total probability and considering both lateral and vertical protection levels, $I_{H1j,req}$ can be expanded as:

$$\begin{aligned} I_{H1j,req} = \big[&P\{|\hat{v}_{nav} - v| > VPL_{1j}|H_{1j}, CF\} \\ &+P\{|\hat{l}_{nav} - l| > LPL_{1j}|H_{1j}, CF\} \\ &-P\{|\hat{v}_{nav} - v| > VPL_{1j} \cap |\hat{l}_{nav} - l| > LPL_{1j}|H_{1j}, CF\} \\ &P(CF|H_{1j})P(H_{1j}) \\ &+\big[P\{|\hat{v}_{nav} - v| > VPL_{1j}|H_{1j}, IF\} \\ &+P\{|\hat{l}_{nav} - l| > LPL_{1j}|H_{1j}, IF\} \\ &-P\{|\hat{v}_{nav} - v| > VPL_{1j} \cap |\hat{l}_{nav} - l| > LPL_{1j}|H_{1j}, IF\}\big] \\ &P(IF|H_{1j})P(H_{1j}) \end{aligned} \quad (2)$$

where v and l are the true vertical and lateral position components, $\hat{v}_{nav}$ and $\hat{l}_{nav}$ are the vertical and lateral position estimates from the navigation algorithm, VPL_{1j} and LPL_{1j} are the vertical and lateral protection levels under H_{1j} hypothesis, and *CF* and *IF* represent correct and incorrect fix events, respectively.

To simplify (2), we conservatively assume that the probability of the lateral and vertical errors exceeding the alert limits conditioned on correctly fixing the ambiguities is zero. Also, assume that all incorrect fixes cause the estimate errors to exceed the protection levels, which leads to $P\{|\hat{v}_{nav} - v_{truth}| > VPL_0|H_0, IF\} = 1$ and $P\{|\hat{l}_{nav} - l_{truth}| > LPL_0|H_0, IF\} = 1$ and as a result, $P\{|\hat{v}_{nav} - v_{truth}| > VPL_0 \cap |\hat{l}_{nav} - l_{truth}| > LPL_0|H_0, IF\} = 1$. Therefore, (2) can be simplified to:

$$\begin{aligned} I_{H1,req} = &P\{|\hat{v}_{nav} - v| > VPL_{1j}|H_{1j}, CF\} \\ &P(CF|H_{1j})P(H_{1j}) \\ &+P\{|\hat{l}_{nav} - l| > LPL_{1j}|H_{1j}, CF\} \\ &P(CF|H_{1j})P(H_{1j}) + P(IF|H_{1j})P(H_{1j}) \end{aligned} \quad (3)$$

Throughout the derivations in this paper, the vertical component of the position error is used exclusively because it is usually the most stringent for precision aviation applications and, if needed, the lateral components can be treated similarly. By dividing the allocation equally in (3) to vertical and lateral (only vertical is shown) and knowing that correct and incorrect fix events are mutually exclusive and exhaustive events $P(IF|H_0) = 1 - P(CF|H_0)$, the vertical allocation of (3) becomes:

$$\begin{aligned} I_{vH1j,req} = &P\{|\hat{v}_{nav} - v| > VPL_{1j}|H_{1j}, CF\} \\ &P(CF|H_{1j})P(H_{1j}) \\ &+\frac{1}{2}\left(1 - P(CF|H_{1j})\right)P(H_{1j}) \end{aligned} \quad (4)$$

The term $P(CF|H_{1j})$ in (4) is the probability of correct fix in the navigation solution conditioned on the hypothesis that receiver *j* has failed. Due to the existence of a fault in the navigation solution, which impacts cycle resolution, it is quite challenging to evaluate this probability. Instead, a solution separation technique is pursued.

Solution separation

Due to the complexity in evaluating $P(CF|H_{1j})$ in (4), we start by rewriting the vertical integrity risk requirement under H_{1j} hypothesis as:

$$I_{vH1j,req} = P\{|\hat{v}_{nav} - v| > VPL_{H1j,}|H_{1j}\}P(H_{1j}) \quad (5)$$

As long as we are able to describe the distribution of $\hat{v}_{nav} - v$, the actual estimator used in generating $\hat{v}_{nav}$ is irrelevant. Under the H_{1j} hypothesis, faulted measurements in receiver *j* introduce an error (bias) in the vertical component of the position estimate $\hat{v}_{nav}$. However, the vertical position estimate excluding the j^{th} receiver $\hat{v}_j$ is the best estimate of the fault-free vertical component of the relative position vector. Add and subtracting $\hat{v}_j$ from $\hat{v}_{nav} - v$:

$$\hat{v}_{nav} - v = (\hat{v}_{nav} - \hat{v}_j) + (\hat{v}_j - v) \quad (6)$$

In (6), $(\hat{v}_{nav} - \hat{v}_j)$ is the best estimate of the bias in the vertical position estimate under H_{1j} hypothesis. $(\hat{v}_j - v)$ is the vertical position estimate error under H_{1j} hypothesis. If $\hat{v}_j$ is estimated with cycle resolution, the distribution of $\hat{v}_j - v$ can be bounded by a Gaussian distribution after accounting for the probability of incorrect fix as illustrated in (2).

Substituting (6) in (5) and accounting for cycle resolution probability in a similar fashion as in (2) to (4) yields:

$$I_{vH1j,req} = P\{|(\hat{v}_{nav} - \hat{v}_j)| + |(\hat{v}_j - v)| > VPL_{H1j}|H_{1j}, CF_j\} P(CF_j|H_{1j})P(H_{1j}) + \frac{1}{2}\left(1 - P(CF_j|H_{1j})\right)P(H_{1j}) \quad (7)$$

The difference between (7) and (4) is that $P(CF|H_{1j})$ in (4) is replaced by $P(CF_j|H_{1j})$. Since the latter term is the probability of correct fix under H_{1j} hypothesis (fault-free after excluding receiver *j*), this can be computed for a bootstrap fixing approach using (8) [8].

$$P(CF_j) = \prod_{i=1}^{m}\left[2\Phi\left(\frac{1}{2\sigma_{j,(i|I)}}\right) - 1\right] \quad (8)$$

Where $\sigma_{j,(i|I)}$ is the i^{th} conditional variance, which is defined as the variance of the ambiguity *i* conditioned on the previous ambiguities in the set $I = \{1,2,\ldots,i\text{-}1\}$ being fixed correctly after excluding receiver *j*. $\sigma^2_{j,(i|I)}$ is the (*i*,*i*) element of the diagonal matrix **D** resulting from the $\mathbf{LDL}^T$ decomposition of the floating cycle ambiguity estimate error covariance matrix. *m* is the number of fixed cycle ambiguities. Finally, Φ is the Gaussian cumulative distribution function, which is defined as $\Phi(x) = \int_{-\infty}^{x}\frac{1}{\sqrt{2\pi}}\exp\left(-\frac{1}{2}z^2\right)dz$.

Rearranging the terms in (7),

$$P\{|\hat{v}_{nav} - \hat{v}_j| + |\hat{v}_j - v| > VPL_{H1j}|H_{1j}, CF_j\} = \frac{I_{vH1j,req} - \frac{1}{2}\left(1 - P(CF_j|H_{1j})\right)P(H_{1j})}{P(CF_j|H_{1j})P(H_{1j})} \quad (9)$$

In appendix A, we show that VPL_{H1j} can be computed from (9) as

$$VPL_{H1j} = |\hat{v}_{nav} - \hat{v}_j| + K_{H1j,CF}\,\sigma_{vj} \quad (10)$$

where, σ_j is the standard deviation of the vertical estimate error after excluding receiver *j*,

$$K_{H1j,CF} = \Phi^{-1}\left[\frac{I_{vH1j,req} - \frac{1}{2}\left(1 - P(CF_j|H_{1j})\right)P(H_{1j})}{2\,P(CF_j|H_{1j})P(H_{1j})}\right] \quad (11)$$

and Φ^{-1} is the inverse cumulative distribution function for a Gaussian distribution.

Notice that, in order to compute VPL_{H1j}, it is necessary to have access to the relative position estimates ($\hat{v}_{nav}$ and $\hat{v}_j$) to compute $|\hat{v}_{nav} - \hat{v}_j|$. Therefore, the calculation of VPL_{H1j} requires access to the measurements and needs to be executed epoch by epoch.

Figure 2 shows a high level schematic description of how the algorithm works for two reference receivers. As the figure shows, the algorithm consists of three parallel processes. The main process is the *navigation solution* where measurements from both receivers are used to estimate the position $\hat{v}_{nav}$. The other two side processes, referred to later as *subset solutions* where the faulty receiver is excluded, compute the fault-free position estimate $\hat{v}_j$, σ_{vj} and $P(CF_j|H_{1j})$. The output of all these processes is then fed to the H1 monitor to compute $K_{H1j,CF}$ and VPL_{H1j}. In figure 2, if VPL_{H11} or VPL_{H12} is larger than VAL, the H_1 monitor detected an inconsistency between the navigation solution and the subset solution and as a result sounds an alarm.

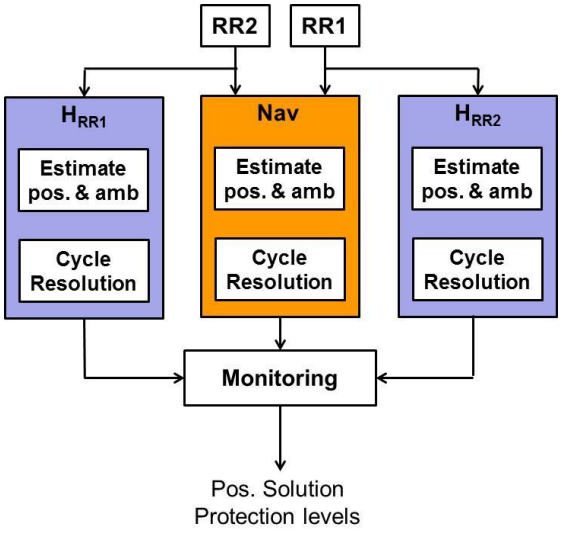

Figure 2 schematic diagram describing H1 monitor processes

PROBABILITY OF FALSE ALARM EVALUATION

If continuity requirements exist, further attention must be paid to the monitor's false alarm rate. (Continuity risk is the probability of a detected but unscheduled navigation function interruption after an operation has been initiated.) Since both $\hat{v}_{nav}$ and $\hat{v}_j$ used in computing VPL_{H1j} in (10) are estimates that are influenced by the measurement noise, they are both random. Therefore, the term $\left|\hat{v}_{nav} - \hat{v}_j\right|$ in (10) is random, which makes VPL_{H1j} a random variable as well. This inherent randomness may cause VPL_{H1j} to exceed *VAL* even under fault-free conditions, which in turn will trigger a false alarm. The probability of false alarm due to the randomness in VPL_{H1j} must comply with the corresponding fault free continuity risk requirement. The likelihood that VPL_{H1j} exceeds *VAL* under fault free condition can be expressed as:

$$C = P\{VPL_{H1j} > VAL | H_0\} P(H_0) \tag{12}$$

In the rest of this derivation, $P(H_0)$ will be dropped because the fault free hypothesis is usually close to 1. Similar to VPL_{H1j}, given a continuity risk budget for the H_{1j} monitor $C_{H1j,req}$, we may compute a stochastic bound that accounts for the randomness in VPL_{H1j}, which we refer to as predictive *VPL* (or $PVPL_{H1j}$ for short) (13).

$$\begin{aligned} &C_{H1j,req} \\ &= P\{\left|\hat{v}_{vnav} - \hat{v}_j\right| + K_{H1j,CF}\,\sigma_{vj} > PVPL_{H1j} | H0\} \end{aligned} \tag{13}$$

The term $K_{H1j,CF}\,\sigma_{vj}$ can be moved to the right hand side of the inequality of (13) because it is nonrandom. Also, adding and subtracting the true vertical position from $\hat{v}_{nav} - \hat{v}_j$, (13) can be rewritten as

$$C_{HRRj,req} = P\{\left|\varepsilon_{vnav} - \varepsilon_{vj}\right| > PVPL'_{H1j} | H0\} \tag{14}$$

where $\varepsilon_{vnav} = \hat{v}_{nav} - v$, $\varepsilon_{vj} = \hat{v}_j - v$ and $PVPL' = PVPL + K_{H1j,CF}\,\sigma_{vj}$. If both the $\hat{v}_{nav}$ and $\hat{v}_j$ solutions are fixed, (14) can be expanded corresponding to all fixing hypotheses using the total law of probability as

$$\begin{aligned} &C_{H1j} \\ &= P\{\left|\varepsilon_{vnav} - \varepsilon_{vj}\right| > PVPL'_{H1j} | CF_{nav}, CF_j, H_0\} \\ &\quad P\{CF_{nav} \cap CF_j\} \\ &+ P\{\left|\varepsilon_{vnav} - \varepsilon_{vj}\right| > PVPL'_{H1j} | CF_{nav}, IF_j, H_0\} \\ &\quad P\{CF_{nav} \cap IF_j\} \\ &+ P\{\left|\varepsilon_{vnav} - \varepsilon_{vj}\right| > PVPL'_{H1j} | IF_{nav}, CF_j, H_0\} \\ &\quad P\{IF_{nav} \cap CF_j\} \\ &+ P\{\left|\varepsilon_{vnav} - \varepsilon_{vj}\right| > PVPL'_{H1j} | IF_{nav}, IF_j, H_0\} \\ &\quad P\{IF_{nav} \cap IF_j\} \end{aligned} \tag{15}$$

Let us conservatively assume that any incorrect fix causes the difference in the vertical estimate error between the navigation and *j*-subset solution to exceed $PVPL'_{H1j}$. Also, since all fixing probabilities $P\{CF_{nav} \cap CF_j\}$, $P\{CF_{nav} \cap IF_j\}$, $P\{IF_{nav} \cap CF_j\}$ and $P\{IF_{nav} \cap IF_j\}$ are mutually exclusive and exhaustive, (15) simplifies to

$$\begin{aligned} &C_{H1j} = \\ &\quad P\{\left|\varepsilon_{vnav} - \varepsilon_{vj}\right| > PVPL'_{H1j} | CF_{nav}, CF_j, H_0\} \\ &\quad P\{CF_{nav} \cap CF_j\} + \left(1 - P\{CF_{nav} \cap CF_j\}\right) \end{aligned} \tag{16}$$

The probability distribution of $\varepsilon_{vnav} - \varepsilon_{vj}$ under H_0 hypothesis is assumed to be a zero mean Gaussian with a variance $\sigma^2_{v,(nav-j)}$. We will derive methods to compute $\sigma^2_{v(nav-j)}$ and $\{CF_{nav} \cap CF_j\}$ shortly, but for now we will use (16) to compute $PVPL'_{H1j}$ as:

$$PVPL'_{H1j} = K_{ff,CF}\,\sigma_{v,(nav-j)} \tag{17}$$

where $K_{ff,CF} = \Phi^{-1}\left[\frac{C_{H1j,req} - (1 - P\{CF_{nav} \cap CF_j\})}{2\,P\{CF_{nav} \cap CF_j\}}\right]$. Using the definition of $PVPL_{H1j}$ from (13) and (14),

$$PVPL'_{H1j} = K_{ff,CF}\,\sigma_{v,(nav-j)} + K_{H1j,CF}\,\sigma_{vj} \tag{18}$$

A continuity breach occurs when any $PVPL_{H1j}$ (for all *j* hypotheses) exceeds *VAL*.

Recall that both $\hat{v}_{nav}$ and $\hat{v}_j$ use common measurements from common reference receivers and possibly from common airborne receivers. Therefore, the estimate errors ε_{vnav} and ε_{vj} are correlated and this correlation must be accounted for when computing $\sigma^2_{v,(nav-j)}$. From the definition of variance,

$$\sigma^2_{v(nav-j)} = E\left\{\left(\varepsilon_{vnav} - \varepsilon_{vj}\right)\left(\varepsilon_{vnav} - \varepsilon_{vj}\right)^T\right\} = \sigma^2_{vnav} - 2\sigma^2_{v(nav,j)} + \sigma^2_{vj} \quad (19)$$

where σ^2_{vnav} and σ^2_{vj} are the vertical estimate error variances for the navigation and *j*-subset solutions, respectively. Assuming that least squares estimates are used for both solutions ([7] provides a detailed method to compute $\sigma^2_{v(nav,j)}$ for the Kalman filter) we may express the estimate error vectors as:

$$\boldsymbol{\varepsilon}_{nav} = (\boldsymbol{H}^T_{nav}\boldsymbol{R}^{-1}_{nav}\boldsymbol{H}_{nav})^{-1}\boldsymbol{H}^T_{nav}\boldsymbol{R}^{-1}_{nav}\boldsymbol{v}_{nav} \quad (20)$$

$$\boldsymbol{\varepsilon}_j = \left(\boldsymbol{H}^T_j\boldsymbol{R}^{-1}_j\boldsymbol{H}_j\right)^{-1}\boldsymbol{H}^T_j\boldsymbol{R}^{-1}_j\boldsymbol{v}_j \quad (21)$$

where **H** is the measurement observation matrix, **R** is the measurement noise covariance matrix and **v** is the measurement noise vector. Therefore,

$$E\left\{\boldsymbol{\varepsilon}_{nav}\boldsymbol{\varepsilon}^T_j\right\} = (\boldsymbol{H}^T_{nav}\boldsymbol{R}^{-1}_{nav}\boldsymbol{H}_{nav})^{-1}\boldsymbol{H}^T_{nav}\boldsymbol{R}^{-1}_{nav} E\left\{\boldsymbol{v}_{nav}, \boldsymbol{v}^T_j\right\}\boldsymbol{R}^{-1}_j\boldsymbol{H}_j\left(\boldsymbol{H}^T_j\boldsymbol{R}^{-1}_j\boldsymbol{H}_j\right)^{-1} \quad (22)$$

$E\{\mathbf{v}_{nav}, \mathbf{v}^T_j\}$ can be derived from the measurement noise covariance matrices for the *nav* and *j* solutions [7]. $\sigma^2_{v(nav,j)}$ is extracted as the (3,3) element of the matrix that results from (22).

The correlation between the ambiguity estimate error vectors in the navigation and *j*-subset solutions must also be accounted for in computing the joint probability $P\{CF_{nav} \cap CF_j\}$. Since both the navigation and *j*-solution estimates are fault free under the H_0 hypothesis, the float ambiguity estimates are unbiased. For an unbiased joint Gaussian, we may underbound this probability, which results in an overbound on $K_{ff,CF}$ in (18) as shown in (23).

$$P\{CF_{nav} \cap CF_j\} \geq P\{CF_{nav}\}P\{CF_j\} \quad (23)$$

Instead of an underbound, we may derive a method to compute $P\{CF_{nav} \cap CF_j\}$ by starting with the definition of a correct fix in the bootstrap fixing method [8]:

$$P\{CF_{nav}\} = P\{|\tilde{\boldsymbol{\varepsilon}}_{N,nav}| \dot{\leq} 0.5\} \quad (24)$$

where,

$\dot{\leq}$ denotes an element-wise operation,

$$\tilde{\boldsymbol{\varepsilon}}_N \triangleq \begin{bmatrix} \hat{\varepsilon}_1 \\ \hat{\varepsilon}_{2|1} \\ \hat{\varepsilon}_{3|1,2} \\ \vdots \\ \hat{\varepsilon}_{m|1,2,\cdots,(m-1)} \end{bmatrix}, \text{ and}$$

$\hat{\varepsilon}_{i|1,\ldots,i-1}$ is the i^{th} conditional ambiguity estimate error, which is defined as ambiguity *i* estimate error conditioned on the previous ambiguities {1,2,…,*i*-1} being fixed. From [8], $\tilde{\boldsymbol{\varepsilon}}_N$ is related to the float ambiguity estimate error vector $\boldsymbol{\varepsilon}_N$ through the matrix **L** resulting from the $\mathbf{LDL}^T$ decomposition of the floating cycle ambiguity estimate error covariance matrix (25).

$$\tilde{\boldsymbol{\varepsilon}}_N = \boldsymbol{L}^{-1}\boldsymbol{\varepsilon}_N \quad (25)$$

Similarly, we may express the probability of correct fix for the *j*-solution ambiguities as:

$$\boldsymbol{P}\{\boldsymbol{CF_j}\} = \boldsymbol{P}\{|\tilde{\boldsymbol{\varepsilon}}_{N,j}| \dot{\leq} \boldsymbol{0.5}\} \quad (26)$$

From the definitions in (24) and (26), we may represent the joint probability of correct fix from both solutions as:

$$\boldsymbol{P}\{\boldsymbol{CF_{nav}} \cap \boldsymbol{CF_j}\} = \boldsymbol{P}\left\{\left|\begin{matrix}\tilde{\boldsymbol{\varepsilon}}_{N,nav} \\ \tilde{\boldsymbol{\varepsilon}}_{N,j}\end{matrix}\right| \dot{\leq} \boldsymbol{0.5}\right\} \quad (27)$$

From (25), write the vector in the inequality of (27) as

$$\begin{bmatrix}\tilde{\boldsymbol{\varepsilon}}_{N,nav} \\ \tilde{\boldsymbol{\varepsilon}}_{N,j}\end{bmatrix} = \begin{bmatrix}\boldsymbol{L}^{-1}_{nav} & \boldsymbol{0} \\ \boldsymbol{0} & \boldsymbol{L}^{-1}_j\end{bmatrix}\begin{bmatrix}\boldsymbol{\varepsilon}_{N,nav} \\ \boldsymbol{\varepsilon}_{N,j}\end{bmatrix} \quad (28)$$

The probability distribution of $\begin{bmatrix}\tilde{\boldsymbol{\varepsilon}}_{N,nav} \\ \tilde{\boldsymbol{\varepsilon}}_{N,j}\end{bmatrix}$ is zero mean multivariate Gaussian with covariance **Q** that can be derived from (28) as:

$$\boldsymbol{Q} = \begin{bmatrix}\boldsymbol{L}^{-1}_{nav} & \boldsymbol{0} \\ \boldsymbol{0} & \boldsymbol{L}^{-1}_j\end{bmatrix}\begin{bmatrix}\boldsymbol{P}_{N,nav} & \boldsymbol{P}_{N,nav\,j} \\ \boldsymbol{P}_{N,j\,nav} & \boldsymbol{P}_{N,j}\end{bmatrix}\begin{bmatrix}\boldsymbol{L}^{-1}_{nav} & \boldsymbol{0} \\ \boldsymbol{0} & \boldsymbol{L}^{-1}_j\end{bmatrix}^{\boldsymbol{T}} \quad (29)$$

where $P_{N,nav}$ and $P_{N,j}$ are the covariance matrices of the float ambiguity estimate error vector for the navigation and *j*-subset solutions, respectively. $P_{N,nav\ j}$ and $P_{N,j\ nav}$ matrices contain the cross covariance between the navigation and *j*-subset solutions for the float ambiguity estimate error vector. These matrices can be extracted corresponding to the ambiguity elements of the matrix that results from (22). As a result, the probability term in (27) can be evaluated efficiently using the multivariate Gaussian cumulative distribution function (*mvncdf*) in MATLAB.

In summary, $P\{CF_{nav} \cap CF_j\}$ is computed using (23) or the multivariate Gaussian cdf function with zero mean, covariance **Q** from (29), and limits at – 0.5 and 0.5. This $P\{CF_{nav} \cap CF_j\}$ is used to compute $K_{FF,CF}$, which is

multiplied by $\sigma_{v(nav-j)}$ from (19) and added to $\left(K_{H1j,CF}\ \sigma_{vj}\right)$ to compute $PVPL_{H1}j$ as shown in (18).

NAVIGATION APPLICATION EXAMPLE

In this section, the H_0 and H_1 performance of a high accuracy and integrity navigation system is quantified through covariance analysis. An example of the navigation algorithms that were developed in [3, 6, 16] is used as a baseline navigation architecture for reference receiver failure detection and mitigation. Next is a summary of the underlying concept of these algorithms. More details can be found in [3, 6, 16].

The GPS navigation algorithm performs geometry-free/divergence-free code-carrier filtering continuously for visible satellites on both the aircraft and the reference station until the aircraft is close to the station [16]. Geometry-free filtering [17], by definition, does not depend on the geometry of the satellites or the user location and eliminates major error sources such as atmospheric errors, clock and ephemeris errors and leaves relatively small errors such as receiver noise and multipath. A geometry free measurement of the widelane cycle ambiguity is formed by subtracting the narrowlane pseudorange from the widelane carrier [17, 18]. A drawback of the geometry free measurement is the presence of higher noise caused by the combination of L1 and L2 carrier phase measurements. This drawback can be overcome by filtering the geometry free measurement over time prior to the final approach. In order to model colored multipath noise in the geometry free measurements, a first order Gauss-Markov measurement error model is used. In this work, a time constant of 100 seconds for the reference station and 30 seconds for aircraft is assumed. The outputs of the filtering process are the floating widelane cycle ambiguity estimates. When the aircraft is close to the reference station, floating widelane cycle ambiguity estimates can be estimated accurately with the aid of satellite geometric redundancy [3, 6, 16] and are then fixed subject to the integrity risk requirements using the bootstrap method [8].

This analysis is conducted for a single aircraft approach by covariance analysis. To account for the GPS satellite geometry change, the covariance analysis is performed by simulating 1440 approaches (one approach per minute during the day). For each approach, σ_{vnav}, σ_{vj}, probability of correct fix, K values and $\sigma^2_{v(nav-j)}$ are computed. Next, these values are used to compute VPL_{H0} *and* $PVPL_{H1j}$ (using both the loose bound and the accurate evaluation of $P\{CF_{nav} \cap CF_j\}$). The requirements and simulation parameters are based on those given in [5,16]. The standard deviation of the raw carrier phase measurement noise is assumed to be 7 mm and the standard deviation of the raw pseudorange measurement noise is assumed to be 35 cm. The remaining simulation parameters are summarized in Table 1.

Table 1: Example Simulation Parameters

Parameter	Value
$I_{vH0,req}$	6×10^{-7}
$I_{vH1j,req}$	1×10^{-7}
$P(H_{1j})$	1×10^{-5}
Continuity risk req.	1×10^{-6}
Satellite constellation	24 SV (DO-229) [10]
Number or RR	2
Location	Atlantic Ocean (37^oN and 74^oW)
Maximum airborne prefiltering time	5 minutes

Using the simulation parameters in Table I, figure 3 shows VPL_{H0} and both the tight and loose bounds of $PVPL_{H1}$. Notice that VPL_{H1} is not computed in this analysis because it requires access to the measurements and this is only a covariance analysis. In addition, VPL_{H1} acts as a test statistic for the $H1$ monitor and by design it meets the allocated $H1$ integrity risk requirements. The false alarm probability of the monitor is evaluated by computing $PVPL_{H1}$ that is shown in Figure 3. The figure also illustrates that $PVPL_{H1}$ is always larger than VPL_{H0} for the parameters in Table 1, which illustrates that the continuity risk requirement for the $H1$ filter is more demanding than the fault free integrity risk requirement. It also shows that the loose bound on $PVPL_{H1}$ is almost the same as the tight bound. Therefore, it is justified for this example and the parameters in Table 1 to use the simpler loose bound of $PVPL_{H1}$ without sacrificing performance. This however, should be treated on a case-by-case basis if other parameters or algorithms are to be implemented.

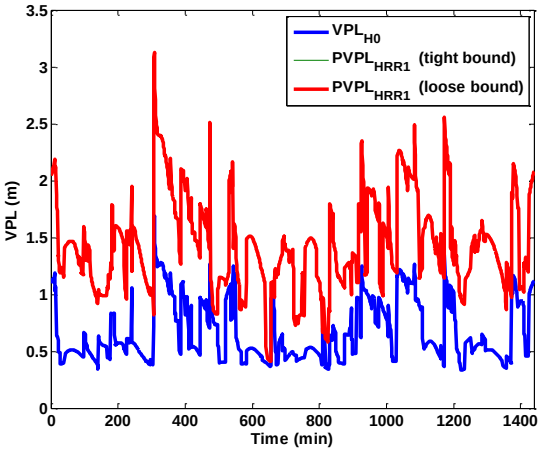

Figure 3: $VPLH_0$ and VPL_{H1} curves over 24 hour period

CONCLUSIONS

In this paper, we developed a monitor that detects single reference receiver failures using solution separation for carrier phase navigation architectures that rely on cycle resolution. VPL and PVPL equations have been derived to meet specific integrity and continuity risk allocations. These derivations account for correlation between different solutions in the solution separation process and can provide both tight and loose bounds on PVPL. In the future, this work will be extended to address the isolation of the faulty receiver and its impact on integrity and continuity risks.

APPENDIX A: VPL FORMULA DERIVATION

This appendix provides a derivation of computing VPL_{H1j} from an allocated requirement I_{H1req}., for a random variable ε_v that is Gaussian distributed with a mean m and standard deviation σ_v:

$$P\{|\varepsilon_v| > VPL_{H1j}\} = I_{h1jreq} \tag{30}$$

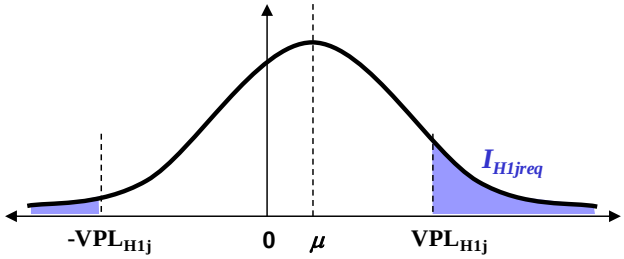

Figure 4: A schematic representation of a biased Gaussian distribution including the area that represents the integrity risk requirement I_{H1jreq}.

From Figure 4, (30) can be written in terms of the Gaussian cdf Φ as,

$$\Phi\left(\frac{-VPL_{H1j}-\mu}{\sigma_v}\right) + 1 - \Phi\left(\frac{VPL_{H1j}-\mu}{\sigma_v}\right) = I_{H1jreq} \tag{31}$$

Although, it is quite difficult to solve for VPL_{H1j} analytically from (31), a conservative quantity can be derived. Consider first the case where μ is positive as in Figure 4. In that case, the area of I_{H1jreq} that is under the positive tail will always be larger than the one under the negative tail. Also, it can be easily shown that the area under the positive tail corresponding to I_{H1jreq} is larger than half of the total area of I_{H1jreq}. Therefore, as illustrated in Figure 5, (31) can be simplified and converted to a one-sided tail with $I_{H1jreq}/2$ and used to compute a conservative value for VPL_{H1j} as,

$$1 - \Phi\left(\frac{VPL'_{H1j}-\mu}{\sigma_v}\right) = \frac{I_{H1jreq}}{2} \tag{32}$$

which can be used to solve for the conservative VPL'_{H1j} (33).

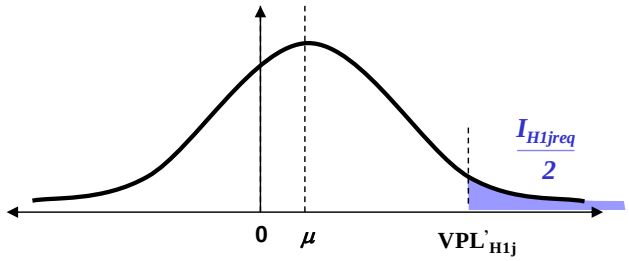

Figure 5: A schematic representation of the conservative VPL'_{H1j} that is based on one sided tail probability of $I_{H1jreq}/2$.

$$VPL'_{H1j} = \mu - \Phi^{-1}\left(\frac{I_{H1jreq}}{2}\right)\sigma_v = \mu + K\,\sigma_v \tag{33}$$

where $K = -\Phi\left(\frac{I_{H1jreq}}{2}\right)$

For negative μ, the same logic can be followed, and VPL'_{H1j} in that case becomes $VPL'_{H1j} = -\mu + K\,\sigma_v$. As a result, for any value of μ, VPL_{H1j} can be written as,

$$VPL'_{H1j} = |\mu| + K\,\sigma_v \tag{34}$$

ACKNOWLEDGMENT

The authors gratefully acknowledge the Naval Air Systems Command (NAVAIR) of the US Navy for supporting this research. The authors would like to specifically acknowledge the feedback and guidance of Marie Lage regarding this work. However, the opinions discussed here are those of the authors and do not necessarily represent those of the U.S. Navy or any other affiliated agencies.

REFERENCES

[1] "Minimum Aviation System Performance Standards for the Local Area Augmentation System Airborne Equipment," *RTCA Document Number DO-245A*, December 2004.

[2] J. Hansen, G. Romrell, N. Nabaa, R. Andersen, L. Myers, and J. McCormick, "DARPA Autonomous Airborne Refueling Demonstration Program with Initial Results," *Proceedings of the 19th International Technical Meeting of the Satellite*

Division of the Institute of Navigation ION GNSS 2006, Fort Worth, TX, Sep. 2006.

[3] S. Khanafseh and B. Pervan. "Autonomous Airborne Refueling of Unmanned Air Vehicles Using the Global Positioning System," *Journal of Aircraft*, Vol. 44, No. 5, Sep.-Oct. 2007.

[4] S. Dogra, J. Wright, and J. Hansen, "Sea-Based JPALS Relative Navigation Algorithm Development," *Proceedings of the 18th International Technical Meeting of the Satellite Division of the Institute of Navigation ION GNSS 2005*, Long Beach, CA, Sept. 2005.

[5] S. Wu, S. Peck and R. Fries, "Geometry Extra-Redundant Almost Fixed Solutions: A High Integrity Approach for Carrier Phase Ambiguity Resolution for High Accuracy Relative Navigation," *Proceeding of the IEEE/ION Position, Location, and Navigation Symposium (PLANS '2008)*, Monterey, CA, Apr. 2008.

[6] M. Heo, B. Pervan, S. Pullen, J. Gautier, P. Enge, and D. Gebre-Eziabher, "Robust Airborne Navigation Algorithm for SRGPS," *Proceedings of IEEE/ION Position, Location, and Navigation Symposium (PLANS '2004)*, Monterey, CA, Apr. 2004.

[7] S. Khanafseh and B. Pervan, "Detection and Mitigation of Reference Receiver Faults in Differential Carrier Phase Navigation Systems", IEEE Transactions on Aerospace and Electronic Systems, Vol. 47, No. 4, 2011, pp. 2391-2404.

[8] P. Teunissen, "GNSS Ambiguity Bootstrapping: Theory and Application," *Proceeding KIS2001, International Symposium on Kinematic Systems in Geodesy, Geomatics and Navigation*, Banff, Canada, 2001.

[9] P. Teunissen, "Integer Estimation in the Presence of Biases," Journal of Geodesy, No. 75, 2001, pp. 399-407.

[10] Khanafseh, S., Joerger, M., Pervan, B., "Integrity Risk of Cycle Resolution in the Presence of Bounded Faults," Proceedings of IEEE/ION PLANS 2012, Myrtle Beach, South Carolina April 2012, pp. 664-672.

[11] Khanafseh, Samer, Joerger, Mathieu, Pervan, Boris, Von Engeln, Axel, "Accounting for Tropospheric Anomalies in High Integrity and High Accuracy Positioning Applications," Proceedings of the 24th International Technical Meeting of The Satellite Division of the Institute of Navigation (ION GNSS 2011), Portland, OR, September 2011, pp. 513-522.

[12] B. Pervan, S. Pullen, and J. Christie, "A Multiple Hypothesis Approach to Satellite Navigation Integrity," *NAVIGATION: Journal of Institute of Navigation*, vol. 45, No. 1, Spring 1998.

[13] F. Liu, T. Murphy, and T. Skidmore, "LAAS Signal-in-Space Integrity Monitoring Description and Verification Plan," *Proceedings of the 10th International Technical Meeting of the Satellite Division of the Institute of Navigation ION GPS 1997*, Kansas City, MO, Sept. 1997.

[14] R. Brown, "A Baseline RAIM Scheme and a Note on the Equivalence of Three RAIM Methods," *NAVIGATION: Journal of The Institute of Navigation*, vol. 39, No. 3, Fall 1992.

[15] B. Parkinson, and P. Axelrad, "Autonomous GPS Integrity Monitoring Using the Pseudorange Residual," *NAVIGATION: Journal of The Institute of Navigation*, vol. 35, No. 2, 1988.

[16] S. Langel, S. Khanafseh, F. C. Chan, and B. Pervan, "Cycle Ambiguity Reacquisition in UAV Applications Using a Novel GPS/INS Integration Algorithm," *Proceedings of the International Technical Meeting of the Satellite Division of the Institute of Navigation ION-ITM 2009*, Anaheim, CA, Jan. 2009.

[17] G. A. McGraw, "Generalized Divergence-Free Carrier Smoothing with Applications to Dual Frequency Differential GPS," *NAVIGATION: Journal of Institute of Navigation*, Vol. 56, No. 2, Summer 2009.

[18] P. Misra and P. Enge, *Global Positioning System signals, Measurements, and Performance*. Lincoln, MA: Ganga-Jamuna Press, 2001.